COLLAPSE BY PONDING OF SHELLS†

S. A. Lukasievicz‡

Warsaw Technical University, Poland,

and

P. G. Glockner

Department of Mechanical Engineering, The University of Calgary, Calgary, Alberta, Canada

Abstract—The problem of stability of shells of positive Gaussian curvature subjected to a concentrated load, internal or external pressure and an accumulating ponding fluid in the depression caused by the load is the subject of this paper. Critical values of the load are calculated by a so called "geometrical method", using variational Lagrangian principles. The shape of the shell is assumed to be nearly isometrical to the initial shape and its bending rigidity is taken into account. Simple relations for the critical load are obtained and the results presented in graphical form. The expressions and diagrams presented facilitate calculation of critical loads and describe the behaviour of the shell undergoing very large deflections.

1. INTRODUCTION

The problems of large deflection and stability of elastic shells are usually treated on the basis of simplified equilibrium and compatibility equations of the theory of shells, as for example, Donnell's nonlinear equations, solved by means of Ritz or Galerkin methods.

Solutions for analogous problems for thin membranes, where bending ridigity of the shell is neglected, have also been obtained by solving simplified equations of equilibrium. In most cases, the solution of exact equations is possible only if the treatmentis restricted to "small deflections". Problems of ponding instability of a membrane have also been solved[1] using linear membrane equations of equilibrium with the assumption that the ponding region is small and the pond is shallow so that linear membrane theory is applicable.

In this paper, a non-classical geometrical method of analysis is used. The characteristic mode of deflections observed in experiments on shells and membranes undergoing large deflections, involve deformation patterns which are very similar to the isometrically transformed surface, i.e. a surface in which the metric tensor remains unchanged.

Here we approximate the post-buckling deflection pattern by a surface which is quasi-isometric to the initial one. Since the Gaussian curvature of the isometrically deformed surface must be equal to the curvature of the initial surface, the deformed surfaces are easily predicted. In the case of an arbitrary shell of double curvature, with curvatures κ_1 and κ_2, the deformed shape can be approximated by a segment of a paraboloid. In the case of a sphere, the deformed shape must also be a sphere of the same curvature. We can assume, therefore, that the deflection has the approximate shape presented in Fig. 1 and consists of a dimple together with a ridge along which the shell is undergoing severe bending.

2. SHELL OF POSITIVE GAUSSIAN CURVATURE

Consider a shell of positive double curvature (Fig. 1) under the action of a concentrated force, P, an internal pressure, q and the weight of a ponding fluid of weight density, γ, which is accumulating in the depression caused by load. The local undeformed shape of the shell in the vicinity of the ponding region is described by a paraboid with constant radii of curvatures, R_1 and R_2, measured at the point of application of the load. The deformed shape is a mirror-like reflection of the original shape. Only one unknown parameter, the depth of the depression, defines the shape of the shell after deformation, which can easily be found using a Lagrangian variational principle
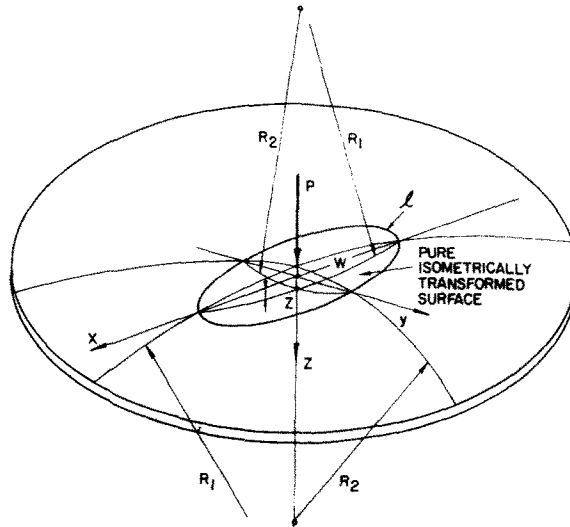
$$\delta W = 0, \tag{1}$$

Fig. 1. Shape of positive Gaussian curvature shell after deformation.

where W is the potential energy of the system, consisting of the work done by the external loads and the strain energy of the shell.

Assume that the deformation of shell surface is so small that it can be described by the relation

$$z = \frac{1}{2}(\kappa_1 x^2 + \kappa_2 y^2),$$

where $\kappa_1 = 1/R_1$ and $\kappa_2 = 1/R_2$ are the arbitrary curvatures of the middle surface at the point of maximum deflection. The line, l, describing the ridge on the shell surface is an ellipse with half-axes

$$a = \sqrt{(w_{max} \cdot R_1)}, \quad b = \sqrt{(w_{max} \cdot R_2)},$$

the equation of which is given by

$$x = a \cos(t), \quad y = b \sin(t),.$$

where t is a parameter.

The energy associated with the change in geometry takes the following simple form [2]

$$U = \pi c \, Eh^{5/2} \, w_{max}^{3/2} (\kappa_1 + \kappa_2), \tag{2}$$

where E is Young's modulus and h is the thickness of the shell. The maximum stress in the ridge region is [2]

$$\sigma = c' \, Eh^{1/2} \, w_{max}^{1/2} \sqrt{(\kappa_1 \kappa_2)}, \tag{3}$$

where c and c' are constant coefficients, $c = 0.19$, $c' = 0.9$.

The work done by the concentrated force, P, applied at point D is given by

$$A = P \, w_{max} = 2P \cdot f, \tag{4}$$

while the work done by the ponding fluid can be calculated as

$$L(\gamma) = \int_0^{y_c} Q_w \, dy, \tag{5}$$

where Q_w is the weight of the fluid given by

$$Q_w = \frac{\pi \gamma f^2}{\sqrt{(\kappa_1 \kappa_2)}},$$ (6)

and where γ denotes the density of the fluid and $w_{max} = 2f$ is the maximum deflection of the shell.

The displacement of the center of gravity of the ponding fluid is found, approximately, from Fig. 1 as

$$y_c = f + kf,$$ (7)

where k is the coefficient defining the position of the center of gravity of the segment of theparaboloid given by

$$z = \frac{1}{2}\left(\frac{x^2}{R_1} + \frac{y^2}{R_2}\right).$$

Introducing Q_w from eqn (6) we find, after integration of eqn (5)

$$L(\gamma) = \frac{1}{3}(1+k)\pi\gamma\sqrt{(R_1 R_2)}\,f^3 = \frac{1}{24}(1+k)\pi\frac{1}{\sqrt{(\kappa_1 \kappa_2)}}\,w^3.$$ (8)

The work done by the internal pressure, q, is written as

$$L(q) = \frac{\pi}{2}\,w^2\,q\,\frac{1}{\sqrt{(\kappa_1 \kappa_2)}}.$$ (9)

Thus, the total potential energy of the system, W, is given by

$$W = \pi c E h^{5/2} w^{3/2}(\kappa_1 \kappa_2) + \frac{\pi}{2}\,w^2 q\,\frac{1}{\sqrt{(\kappa_1 \kappa_2)}}$$

$$-Pw - \frac{1}{24}(1+k)\pi\gamma\frac{1}{\sqrt{(\kappa_1 \kappa_2)}}\,w^3,$$ (10)

and condition (1) takes the form

$$\delta W = \frac{3}{2}\,\pi c E h^{5/2} w^{1/2}(\kappa_1 + \kappa_2)\mathrm{d}w + \pi q\,\frac{1}{\sqrt{(\kappa_1 \kappa_2)}}\,w\,\mathrm{d}w$$

$$-P\mathrm{d}w - \frac{1}{8}(1+k)\,\pi\,\gamma\frac{1}{\sqrt{(\kappa_1 \kappa_2)}}\,w^2\mathrm{d}w = 0.$$ (11)

The force P which can be applied to the system is obtained as

$$P = \frac{3}{2}\,\pi c E h^{5/2}(\kappa_1 + \kappa_2)\sqrt{(w)} + \pi q\,\frac{1}{\sqrt{(\kappa_1 \kappa_2)}}\,w$$

$$-\frac{1}{8}(1+k)\,\pi\,\gamma\frac{1}{\sqrt{(\kappa_1 \kappa_2)}}\,w^2.$$ (12)

The maximum value of this load, $P = P_{cr}$, can be obtained from

$$\frac{\partial P}{\partial w} = 0,$$

which results in

$$\frac{3}{2} \pi c \, Eh^{5/2}(\kappa_1 + \kappa_2) \frac{1}{2\sqrt{(w)}} + \pi q \frac{1}{\sqrt{(\kappa_1 \kappa_2)}} +$$

$$-\frac{1}{4}(1+k) \pi \gamma \frac{1}{\sqrt{(\kappa_1 \kappa_2)}} w = 0. \tag{13}$$

Solving eqn (13) we find the value of w corresponding to the value of P, which when introduced into eqn (12), results in the value of the cirtical load.

Introduce the following notations:

$$P_c = \frac{3 \pi Eh^3 (\kappa_1 + \kappa_2)}{2}, \quad q_c = \frac{E h^2}{3(1-\nu^2)} \sqrt{(\kappa_1 \kappa_2)} (\kappa_1 + \kappa_2),$$

$$\gamma_c = \frac{12 \, Eh}{(1+k)} \sqrt{(\kappa_1 \kappa_2)} (\kappa_1 + \kappa_2), \quad x = \sqrt{(w/h)}. \tag{14}$$

With this notation, the above relation can be presented in a simpler form as

$$\frac{P}{P_c} = cx + \frac{q}{q_c} \frac{2}{3\sqrt{3(1-\nu^2)}} x^2 - \frac{\gamma}{\gamma_c} x^4$$

$$x^3 = \frac{\gamma_c}{\gamma} \frac{c}{4} + \left(\frac{q}{q_c}\right)\left(\frac{\gamma_c}{\gamma}\right) \frac{1}{3\sqrt{3(1-\nu^2)}} x. \tag{15}$$

For the spherical shell $\kappa_1 = \kappa_2 = \frac{1}{R}$ and

$$P_c = \frac{3\pi Eh^3}{R}, \quad \gamma_c = \frac{24 \, Eh}{(1+k)R^2}, \quad q_c = \frac{2E}{\sqrt{3(1-\nu^2)}} \left(\frac{h^2}{R^2}\right). \tag{16}$$

Equations (15) can be solved inclosed form.

Results from the solution of the above set of equations are presented in Figs. 2–4. The results
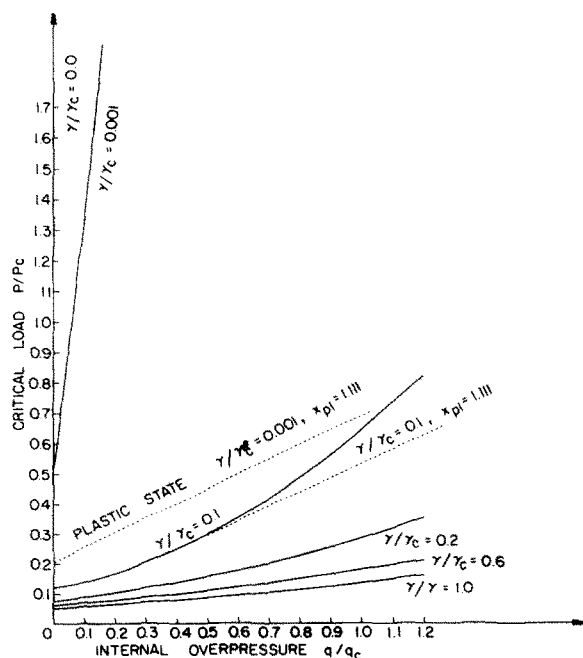

Fig. 2. Critical load as a function of internal pressure for different fluid densities.
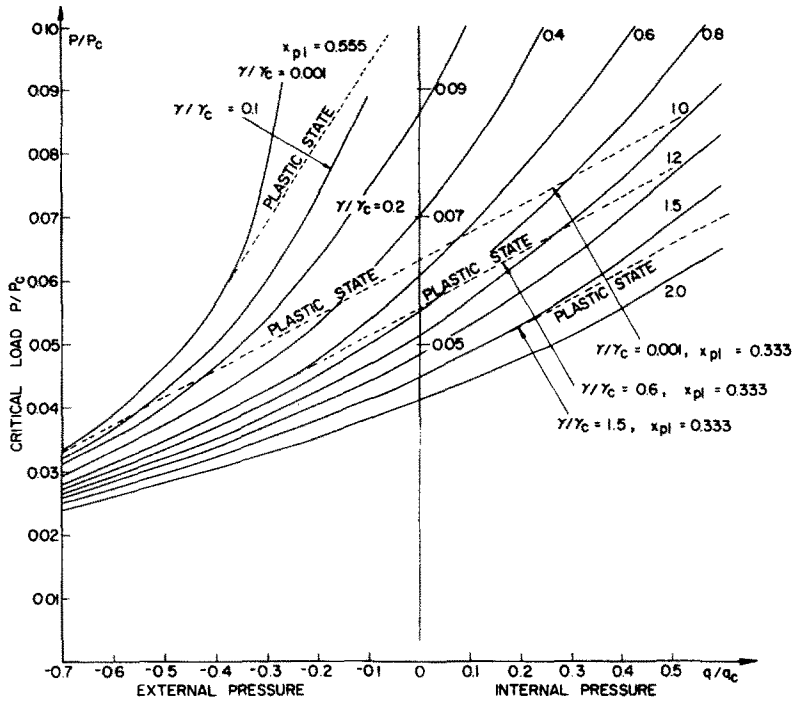
Fig. 3. Critical load as a function on internal and external pressure for different fluid densities.

indicate the nonlinear effect of internal pressure and density on the critical load which is similar to that observed for the elastic membrane. However, for $q = 0$, the critical load P is now finite in contrast to the results obtained for the elastic membranes.

The relation between the non-dimensionalized force P/P_c and the non-dimensionalized displacement function, $x = \sqrt{(w/h)}$, is presented in Fig. 5 for different values of non-dimensional densities, γ/γ_c, and pressures, q/q_c. We observe that if the fluid density is small and the shell is under a large external pressure the critical value of the load, P, is very small and is accompanied by small deflections. Internal pressure in the shell increases the value of P substantially so that at large internal pressures, (e.g. $q/q_c = 1.0$, $\gamma/\gamma_c = 0.1$) the maximum value of the force P occurs after pliastification of the ridge area of the shell ($E/\sigma_{p1} = 500$ and
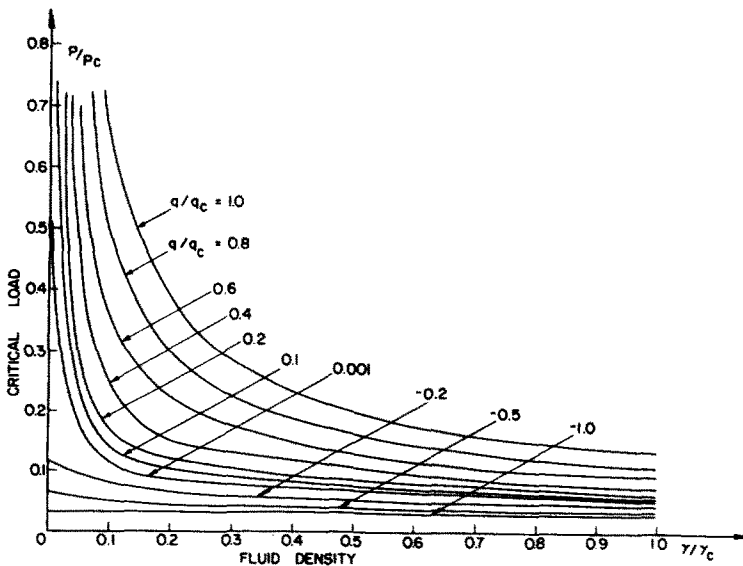

Fig. 4. Critical load as a function on fluid density for different values of pressure.
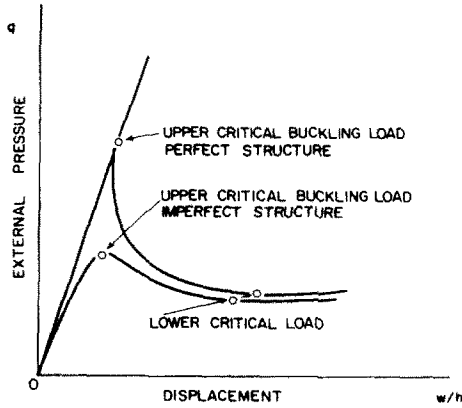
Fig. 5. Concentrated force as a function of deflection for different values of the load.

$h/R = 1/500$) and cannot be taken to be the actual or real critical force. Assuming that the movement of the ridge over the surface of the shell is limited by the plastic deformations in the ridge area (when plastic deformation appears, the strain energy rapidly increases), we obtain from eqn (3)

$$x = \sqrt{\left(\frac{w}{h}\right)} = \frac{\sigma_{p1}}{c' \, Eh \, \sqrt{(\kappa_1 \kappa_2)}} = x_{p1}, \tag{17}$$

where σ_{p1} is the yield stress. Introducing this value of x into eqn (18) we find the force $(P/P_c)_{p1}$, corresponding to the onset of yielding in the shell, presented in Figs. 3 and 4 by dotted straight lines. If we assume that for steel shells the ratio $E/\sigma_{p1} \simeq 500$, we find for a spherical shell the value

$$x_{p1} = 0.222 \times 10^{-2} \, R/h,$$

which depends only on the ratio R/h. If, e.g. $R/h = 500$, $x_{p1} = 1.111$, a value presented in Fig. 5 by a vertical straight line.

3. SPHERICAL SHELL

Next consider the case of a spherical shell under the action of zero concentrated force, and external pressure, $q_e = -q$ and ponding fluid with density γ. Then, for eqn (15) we obtain,

$$q_e = 3 \left[\frac{c}{x} - \frac{\gamma}{\gamma_c} x^2\right] \left(\frac{h}{R}\right)^2 E. \tag{18}$$

The upper buckling load, q_c, (see Fig. 6 for definitions of upper and lower buckling loads of perfect and imperfect structures) cannot be obtained from the above derived expression. We note that for $x \to 0$, $q_e \to \infty$, eqn (18) defines the maximum equilibrium pressure for a shell in which the deformation patterns are already developed, the existence of which is assumed in deriving eqn (2). Thus, only the lower buckling load is obtainable from this analysis. However, we note that equilibrium of the shell under such loading conditions is not stable, i.e. if the deflection increases, the external pressure, q_e, decreases to zero. The increase in displacements can be limited by the boundary conditions or by the finite elastic properties of the aterial. In the latter case, stable equilibrium can be defined on the basis of a maximum stress. Introducing x from eqn (17) we find

$$q_e = 3 \left[cc' \left(\frac{Eh}{\sigma_{p1} R}\right) - \frac{1}{c'^2} \frac{\gamma}{\gamma_c} \left(\frac{\sigma_{p1}}{E} \frac{R}{h}\right)^2\right] \frac{h^2}{R^2} E. \tag{19}$$
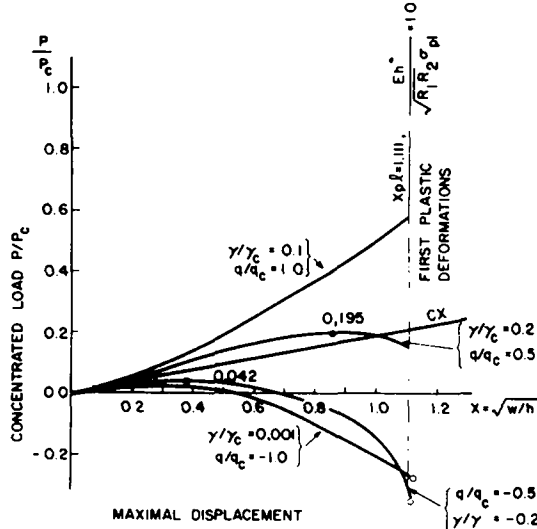
Fig. 6. Definition of lower and upper buckling loads.

The classical value of the critical pressure is usually presented in the form

$$\check{q} = \frac{q}{2E}\left(\frac{R}{h}\right)^2 = \frac{1}{\sqrt{3(1-\nu^2)}} \approx 0.6 \text{ for } \nu = 0.3.$$

Presenting our result in the same form, we have

$$\check{q} = \frac{q_e}{2E}\left(\frac{R^2}{h^2}\right) = \frac{3}{2}\left[cc'\left(\frac{Eh}{\sigma_{p1}R}\right) - \frac{1}{c'^2}\left(\frac{\gamma}{\gamma_c}\right)\left(\frac{\sigma_{p1}R}{Eh}\right)^2\right], \tag{20}$$

which is presented in Fig. 7, $\check{q}\sqrt{3(1-\nu^2)}$ as a function of R/h and for $\gamma = 0$ and $E/\sigma_{p1} = 800$. Many experimental investigations performed for $\gamma = 0$ pointed out that $0.1 \leq \check{q}\sqrt{3(1-\nu^2)} \leq 1.0$ and that it depends on (R/h), [6] and the initial imperfections. The (R/h) dependence has not been confirmed by theoretical investigations on elastic stability of shells. We note that such dependence is obtained from eqn (20) and that for thin shells, the predictions show quite good agreement with experimental data concerning lower values of the critical buckling loads. For
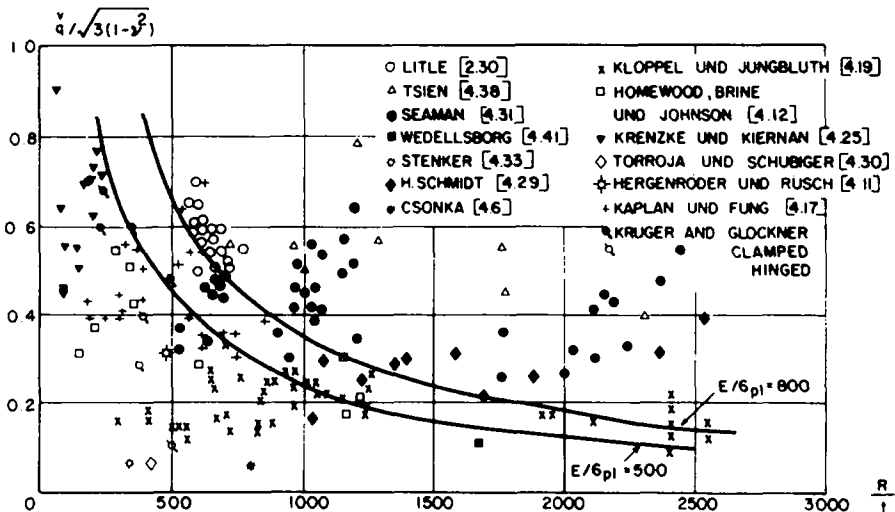

Fig. 7. Comparison of results obtained with experimental data.

thick shells, $R/h < 200$, the agreement is not satisfactory. It should be pointed out that the results of the experiments presented in Fig. 7 were obtained using models of various geometries and initial imperfections and made of a variety on materials. Most often they were made of aluminum or copper for which the ratio E/σ_{p1} can vary between the limits 250 and 2500.

If the external pressure, q and the concentrated force, P, are zero, the critical value of γ/γ_c corresponding to the onset of yielding can be found from eqn (15) as

$$\left(\frac{\gamma}{\gamma_c}\right)_{cr} = \frac{c}{x_{pl}^3} = cc'^3 \left(\frac{Eh}{\sigma_{p1}R}\right).$$ (21)

For $E/\sigma_{p1} = 500$ and $h/R = 1/500$, we have

$$\left(\frac{\gamma}{\gamma_c}\right)_{pl} = cc'^3 = 0.1385.$$

If we neglect the effect of the ponding fluid, i.e. assume $\gamma = 0$, one obtains from eqns (15)

$$\frac{P}{P_c}\frac{q_e}{q_c} = \frac{3}{8} c^2 \sqrt{3(1-\nu^2)}.$$ (22)

This result is derived on the assumption of infinite elastic properties of the shell material. We note that for $P = 0$, $q_{cr} \rightarrow \infty$, which is impossible. However, one should remember that eqn (22) gives only the lower critical load when advanced deflection patterns have already developed, which in turn, means that the upper critical load for the case $P \simeq 0$ cannot be obtained from this relation. When $q_e = 0$, no critical behaviour is observed until the symmetrical deformation pattern is changed into a non-symmetrical one. However, a comparison of the results from eqn (22) with experimental data presented in [4] for the case shallow spherical shells with built-in edges, proves that in the range of $q_e/q_c > 0.004$, the agreement is satisfactory (see Fig. 8), although predictions from eqn (22) are lower than the experimental results in [4], thus providing conservative and safe estimates for the critical load. If plastic properties of the material are
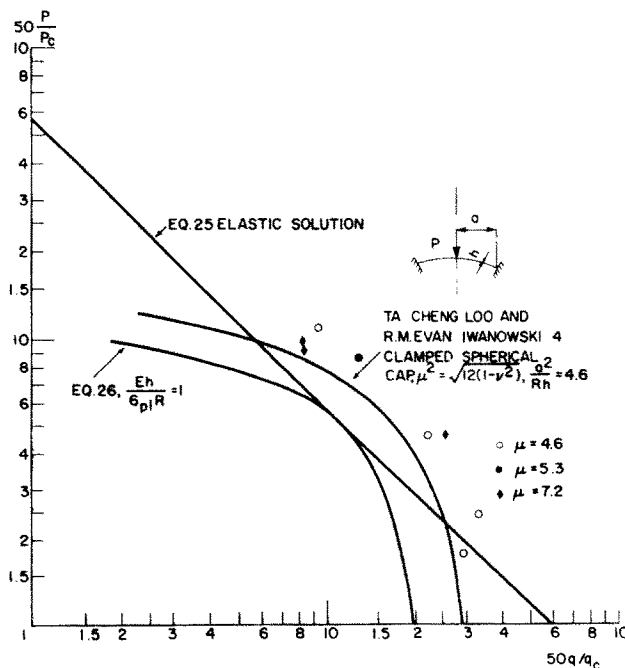

Fig. 8. Comparison of results obtained with results of others.

taken into account, and we assume that the first plastic deformation limits the development of the dimple, we obtain the following relation for the critical force, P/P_c, and q_e/q_c of

$$\frac{P}{P_c} + \frac{2}{3\sqrt{3}(1-2)c'^2} \left(\frac{\sigma_{p1}R}{Eh}\right)^2 \frac{q_e}{q_c} = \frac{c}{c'} \left(\frac{\sigma_{p1}R}{Eh}\right).$$ (23)

Values obtained from this relation are somewhat lower than results in [4]; however, this overall trend, as indicated by the shape of the curve in Fig. 7, is similar.

4. ELASTIC MEMBRANES

In this case the problem becomes much simpler. We obtain from eqn (13) the following the critical force

$$P_c = \pi q \frac{1}{\sqrt{(\kappa_1 \kappa_2)}} w - \frac{1}{8}(1 + k)\pi \gamma \frac{1}{\sqrt{(\kappa_1 \kappa_2)}} w^2.$$ (24)

The condition $\partial P/\partial w = 0$ gives the following equation

$$\frac{\pi q}{\sqrt{(\kappa_1 \kappa_2)}} - \frac{1}{4}(1 + k)\pi \frac{\gamma w}{\sqrt{(\kappa_1 \kappa_2)}} = 0,$$ (25)

from which $w = 4q/(1 + k)\gamma$, and the very simple, closed-form solution is obtained as

$$P_{cr} = \frac{2\pi q^2}{\sqrt{(\kappa_1 \kappa_2)}(1 + k)\gamma},$$ (26)

which for the spherical shell becomes

$$P_{cr} = \frac{2\pi q^2 R}{(1 + k)\gamma}.$$ (27)

Values resulting from eqn (27) are compared with results obtained in [1] by solving the membrane equilibrium equations numerically (see Fig. 9). We note excellent argeement between the two sets of results. The points marked by a^* on the diagram are calculated by means of eqn (27).

If the bending rigidity is neglected a real solution for P_{cr} can be obtained only for $q > 0$. If $q < 0$, i.e. for an externally applied pressure load, equilibrium is possible only if $P < 0$, i.e. when the force P supports the membrane.

5. CONCLUSIONS

A closed-form solution to the problem of the stability behaviour of a shell of double curvature under the simultaneous action of a concentrated force, external or internal pressure and an accumulating ponding fluid is obtained in a very simple manner using a variational principle. The theoretical predictions obtained are compared with the results obtained previously by others for the limiting cases of zero fluid density or zero concentrated force. We note satisfactory agreement of our results with those of previous investigators and conclude that this simplified analysis correctly describes the nonlinear behaviour of the shell under the considered loads.

Discrepancies, if any, are due to the simplified relation for the energy in the ridge area (eqn 2). When the thickness of the shell decreases to zero and we deal with a membrane, the agreement with results obtained by others for spherical membranes is excellent. Application of eqn (2) to several problems [2] proved that its accuracy is in many cases satisfactory to obtain results to within 15%. For shells with internal pressure the accuracy of the relations is improved.

The results from this study also point out that the presence of a ponding fluid decreases the critical concentrated load and external pressure, significantly. It would be interesting to compare our results for $\gamma \neq 0$ with experimental data for a shell of double curvature. However, such data is not available to the authors at the present time.
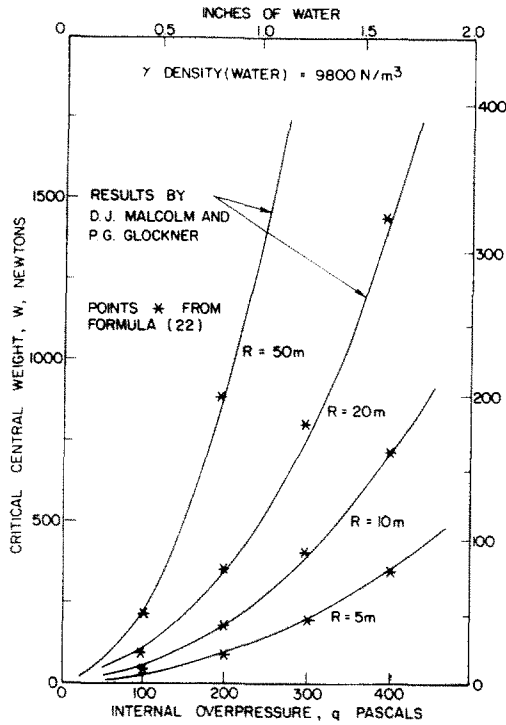
S. A. Lukasiewicz and P. G. Glockner

Fig. 9. Comparison of results obtained for shperical membranes with results of others.

REFERENCES

1. D. J. Malcolm and P. G. Glockner, Collapse by ponding of air-supported membranes. *Proc. ASCE* 104, No. ST9, pp. 1525–1532. Proc. Paper 14002 (1978).
2. A. W. Pogorelov, *Geometricheskie Methody w Nelineynoi Theorii Uprugih Obolochek.* Mockva (1967).
3. S. Lukasiewicz and W. Szyszkowski, Geometryczne Methody Nieliniowej Teorii Powłok. *Proc. II Symp. Shell Structures, Theory and Applications,* Poland, PWN, Warsaw, 1975.
4. Ta-Cheng Loo and R. M. Evan Iwanowski, Interaction fo critical pressures and critical concentrated loads acting on shallow spherical shells. *Trans. ASME* (1966).
5. L. Kollar and E. Dulacska, *Schalenbeulung, Theorie und Ergebnisse der Stabilität Gekrümmter Flächentragwerke.* Verner-Verlag, Düsseldorf (1975).
6. D. S. Kruger and P. G. Glockner, Experiments on the stability of spherical and paraboloidal shells. *Experimental Mech.* 6 (1971).
7. G. A. Thurson and F. A. Penning, Effect of axisymmetric imperfections on the buckling of spherical caps under uniform pressure. *AIAA J.,* 4, (1969).

APPENDIX 1

Calculation of the coefficient k *for the sphere*

This coefficient defines the position of the center of gravity of the ponding fluid, and is defined by the solution, (Fig. 10).

$$x_c = \frac{2}{3} R \frac{\sin^3 \theta}{\theta - \sin \theta \cos \theta}. \tag{A1}$$
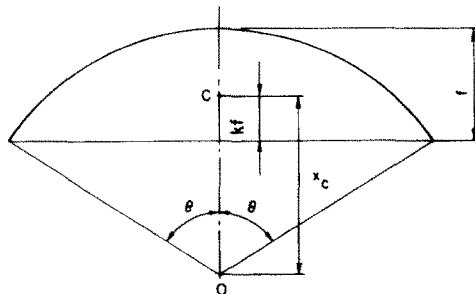
C – CENTER OF GRAVITY

Fig. 10. Position of center of gravity for spherical cup.

Since $\sin \theta = r/R$, $\cos \theta = (R - f)/R$

$$\theta = \arcsin \left(\frac{r}{R}\right) = \frac{r}{R} + \frac{1}{6}\left(\frac{r}{R}\right)^3 + \frac{3}{40}\left(\frac{r}{R}\right)^5 + \ldots$$

and introducing this result into eqn (A1) we find

$$k = \frac{2 + 3f/R}{5 + 3f/R},\tag{A2}$$

and since $f \ll R$, we have $k \cong 0.4$. Calculations performed with the exact solution (A2) proved that the effect of small terms of the order of (f/R) is negligible.